

FILE.

INTERNAL DOCUMENT 171.

I.O.S.

Internal Document No. 171

Calibration of "Hippy" sensors for use in

Wave Energy measurements off S. Uist

aboard the Marex Directional Wave Buoys

*[This document should not be cited in a published bibliography, and is supplied for the use of the recipient only].*

NATURAL ENVIRONMENT  
INSTITUTE OF OCEANOGRAPHIC SCIENCES  
RESEARCH COUNCIL

INSTITUTE OF OCEANOGRAPHIC SCIENCES

Wormley, Godalming,  
Surrey GU8 5UB  
(042-879-4141)

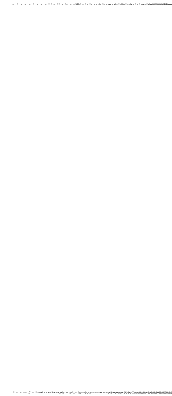
(Director: Dr. A. S. Laughton)

Bidston Observatory,  
Birkenhead,  
Merseyside L43 7RA  
(051-653-8633)

(Assistant Director: Dr. D. E. Cartwright)

Crossway,  
Taunton,  
Somerset TA1 2DW  
(0823-86211)

(Assistant Director: M. J. Tucker)



Internal Document No. 171

Calibration of "Hippy" sensors for use in

Wave Energy measurements off S. Uist

aboard the Marex Directional Wave Buoys

by

G N CRISP

## 1. Introduction

The Marex directional wave buoys which are to be deployed off S. Uist, use "Hippy" sensors to measure the buoys' vertical accelerations. Marex arranged for the predeployment calibration of the sensor to be carried out using the NMI facility at Hythe, and informed IOS of this arrangement.

Since, in use, the vertical acceleration signal will be recorded rather than the heave (displacement) signal, it was proposed to calibrate the accelerometer's signals directly rather than follow the usual practice of recording the heave signal.

Because of the non standard nature of the calibration it was decided that the presence of an IOS scientist, acting as an observer, would be useful.

During the calibrations the author made an independent set of measurements, using an analogue chart recorder, for analysis at Taunton. This short report has two purposes, firstly it describes the calibration technique and the analysis of the resulting data; secondly in the light of the experience gained, a brief discussion of the calibration method is given.

## 2. Calibration Method

2.1 The calibration rig The NMI calibrator consists of a data acquisition system together with a mechanical rig. The rig consists of two parallel bars mounted at their mid points on bearings. With this apparatus a sensor, which is mounted upon a platform at one end between the bars, can be made to describe a vertical circle of 3m diameter at a number of preselected angular speeds. A system of chains and gear wheels maintains the sensor's axis in a constant direction throughout the measurement. This arrangement is illustrated schematically in fig 1. Electrical connections are made to the sensor using flexible wires which are fed out axially through the centre of the main bearings to stationary recording equipment.

The angular speed of the rig is controlled by a servo system employing an electric motor and tachometer which are connected mechanically to the rotating arm by flexible drive belts.

2.2 The recording system The calibration facility incorporates a digital data recording system used to measure the amplitude of the sensor's output and a timing device actuated by a magnet mounted on the rotating arm. This may be used to determine the average angular speed over one rotation. However, for the measurements described here, an analogue chart recorder was used to measure the sensor's output and the angular speed of the rig was determined by timing a number of revolutions using a hand-held stop watch. The calibration of the chart recorder was checked periodically throughout the measurements by injecting known standard voltages and observing the resulting deflections of the pen trace. Both the chart recorder and the digital logging system had input impedances of greater than  $1M\Omega$ , while the specified output impedance of the "Hippy" sensor is  $10\Omega$ ; thus negligible loading of the sensor was expected.

2.3 Calibration Technique With the sensor mounted in the calibration rig the digital logging system was connected across the sensor's output. The rig was set in motion and its angular speed checked at intervals until this became steady. The analogue chart recorder was calibrated on a scale of appropriate sensitivity, by injecting dc voltages, and was then connected across the sensor's output terminals in parallel with the digital recording system. A number of revolutions were timed using a hand-held stopwatch while the chart recorder recorded the sensor's output wave form. Sufficient revolutions were counted so that the total measured time exceeded 100 seconds. This reduces errors in the timing to acceptable levels. Once such a set of measurements had been completed, the rotational speed of the rig was altered and the process repeated. The range of angular speeds used corresponded to a variation in accelerometer output voltage over two orders of magnitude so that several recorder sensitivities had to be used. Whenever the recorder's sensitivity range was altered, the sensor was temporarily disconnected and the recorder was recalibrated on the new range. A record was made of the ambient temperature during the calibrations; this varied over the range  $15^{\circ}$  to  $17^{\circ}\text{C}$ .

#### 2.4 Analysis of chart records

a) Calculation of peak to peak acceleration, The vertical acceleration of the sensor may be calculated provide that it is assumed that the angular speed of the rig is constant throughout each cycle. In this case the vertical displacement of the buoy is given in metres ' by:

$$y = 1.5 \sin\left(\frac{2\pi}{T}\right)t \quad m$$

where T is the rotational period.

So that the vertical acceleration is given by

$$\ddot{y} = -1.5 \left(\frac{2\pi}{T}\right)^2 \sin\left(\frac{2\pi}{T}t\right) \quad \text{ms}^{-2}$$

as the Sin term varies between +1 and -1 the peak to peak excursion of the vertical acceleration has a magnitude of

$$2\left(\frac{2\pi}{T}\right)^2 1.5 \quad \text{ms}^{-2}$$

which on substituting numerical values gives a peak to peak magnitude of

$$\frac{118.44}{T^2} \text{ms}^{-2}$$

b) Measurement of Peak to Peak short amplitudes Owing to the influence of vibrations in the experimental rig, at angular speeds below 0.15 cycles/second, significant high frequency variations were superimposed upon the recorded signals. In order to estimate the peak to peak amplitude of the underlying low frequency sine wave, the average value of the trace at each turning point was estimated by eye. Where possible ten peaks and troughs of the underlying low frequency oscillations were treated in this way and a mean value was then calculated.

3. Results See Tables 1 to 4 below.

TABLE 1      Sensor Serial No 18023

Measure- ment No.	Rotation Period T (seconds)	Signal Amplitude on chart (cm)	Nominal recorder Sensitivity mV/cm	Recorder calibration factor	Peak to peak sensor output (volts)
1	39.22	19.71	4	1.004	0.0792
2	34.29	5.06	20	1.002	0.1013
3	24.51	9.86	20	1.002	0.1975
4	20.13	14.47	20	1.002	0.2899
5	15.20	12.89	40	1.001	0.5162
6	10.31	5.52	200	1.001	1.1053
7	7.77	9.75	200	1.001	1.9527
8	5.94	16.66	200	1.001	3.3368
9	5.12	22.46	200	1.000	4.4924
10	4.34	15.51	400	1.000	6.2056
11	3.83	19.95	400	1.000	7.980

TABLE 2      Sensor Serial No 18024\*

Measure- ment No.	Rotation Period T (seconds)	Signal Amplitude on chart (cm)	Nominal recorder Sensitivity mV/cm	Recorder calibration factor	Peak to peak sensor output (volts)
1	40.37	3.69	20*	1.000	0.0738
2	33.70	5.22	20	1.000	0.1044
3	24.70	9.83	20	1.000	0.1965
4	18.85	17.00	20	1.000	0.3400
5	14.50	14.05	40	1.000	0.5620
6	10.08	5.92	200	0.993	1.1755
7	7.96	9.43	200	0.993	1.8718
8	5.97	16.75	200	0.993	3.3266
9	5.16	22.34	200	0.993	4.4367
10	4.38	15.50	400	0.999	6.1938
11	3.83	20.50	400	0.999	8.1918
12	14.78	13.61	40	0.998	0.5348

\*Sensor 18024 had a dc offset of 0.84 v on its output; in consequence the chart recorder was set to 20 mV/cm maximum sensitivity in order to allow this to be backed off.

TABLE 3 Sensitivity of sensor No 18023

Period (Seconds)	Frequency (Hz)	$\ddot{y}$ m s <sup>-2</sup>	$V_{out}/\ddot{y}$ V/m s <sup>-2</sup>
39.22	0.0255	0.07698	1.028
32.29	0.0310	0.1013	1.006
24.51	0.0408	0.1975	1.001
20.13	0.0497	0.2899	0.992
15.20	0.0658	0.5162	1.006
10.31	0.0970	1.105	0.992
7.77	0.1287	1.953	0.996
5.94	0.1684	3.337	0.994
5.12	0.1953	4.492	0.993
4.34	0.2304	6.206	0.985
3.83	0.2611	7.980	0.990

TABLE 4 Sensitivity of sensor No 18024

Period (seconds)	Frequency (Hz)	$\ddot{y}$ m s <sup>-2</sup>	$V_{out}/\ddot{y}$ V/m s <sup>-2</sup>
40.37	0.0248	0.07268	1.016
33.70	0.0297	0.1043	1.001
24.70	0.0405	0.1941	1.013
18.84	0.0531	0.3335	1.020
14.50	0.0690	0.5634	0.998
10.08	0.0992	1.166	1.008
7.96	0.1256	1.867	1.002
5.97	0.1674	3.320	1.001
5.16	0.1938	4.448	0.997
4.38	0.2281	6.162	1.005
3.83	0.2612	8.077	1.014
14.78	0.0677	0.5422	1.002



#### 4. Analysis of Errors

4.1 Timing errors The accuracy of hand held stop watch measurements is not particularly easy to assess, but it is not unreasonable to assume an uncertainty of  $\pm 0.2$  seconds for each measurement. According to the total time measured, this corresponds to errors in T in the range  $\pm 0.08\%$  to  $\pm 0.13\%$  for the measurements reported here. As the calculated accelerations vary as  $1/T^2$  the resulting errors in sensitivity values calculated from the data are expected to be in about twice this amount, namely  $\pm 0.16\%$  to  $\pm 0.26\%$ .

4.2 Chart recorder Calibration errors The manufacturer's specification for the chart recorder used in this work gives an accuracy of  $\pm 0.2\%$  and, while the calibration procedure used here should compensate for such errors, it is probably not wise to rely on the recorder's linearity to better than this.

#### 4.3 Errors associated with measuring amplitude of short trace

a) Angular frequencies below 0.15Hz At low frequencies, where the absolute accelerations produced by the rotating arm are small, the accelerometers detected high frequency vibrations of significant magnitude as illustrated in Figs 2 and 3. As can be seen, the high frequency "noise" is not random; its magnitude varies cyclically in phase with the rotation of the rig and, in addition, there was evidence on some traces that the high frequency variations were not sinusoidal. Consequently there is considerable uncertainty in estimating the amplitude of the underlying low-frequency sine wave.

In order to estimate the magnitude of the resulting errors a rather conservative approach has been used. The amplitude of the high-frequency variations was estimated by eye, taking account only of the behaviour first at the peaks and then at the troughs on each trace. The error in each observation was defined to be half of the sum of these values. In practice measurement by eye of the trace's underlying amplitude is likely to be more accurate than this, but it is difficult to estimate the degree to which such measurements may be biased by the asymmetrical nature of the high-frequency components in the signal.

b) Angular frequencies above 0.15Hz Above 0.15Hz the influence of vibrations becomes imperceptible in the recordings and the accuracy

of measuring the charts is then governed by the amplitude of the recorded trace. In order to ascribe a magnitude to these errors it had been assumed that the measurements have an intrinsic accuracy of  $\pm 0.5\text{mm}$ .

4.4 Calculation of Overall errors Below 0.15Hz by far the largest contribution to the errors arises from measuring the chart amplitude; as the procedure used to estimate the size of these errors is conservative, no further analysis has been performed and calibration and timing errors have been ignored. Above 0.15Hz it has been assumed for simplicity that each of the proportional errors described above are additive.

Tables 5 and 6 summarise the errors associated with each measurement.

TABLE 5 Sensor 18023

Frequency	$V_{out}/\ddot{y}$	Timing error %	Chart recorder calibration error %	Chart measurement error %	Total *
0.0255	1.028	-	-	+ 6.3	
0.0310	1.006	-	-	+ 4.9	
0.0408	1.001	-	-	+ 4.6	
0.0497	0.992	-	-	+ 3.1	
0.0658	1.006	-	-	+ 8.4	
0.0970	0.992	-	-	+ 3.4	
0.1287	0.996	0.15	+ 0.2	+ 0.7	+ 1.0
0.1684	0.994	0.33	0.2	0.5	+ 1.0
0.1953	0.993	0.26	0.2	0.2	+ 0.7
0.2304	0.985	0.28	0.2	0.3	+ 0.8
0.2611	0.990	0.15	0.2	0.3	+ 0.7

TABLE 6 Sensor 18024

Frequency	$V_{out}/\ddot{y}$	Timing error %	Chart recorder calibration error %	Chart measurement error %	Total *
0.0248	0.07268	-	-	13.5	13.5
0.0297	0.1043	-	-	12.5	12.5
0.0405	0.1941	-	-	9.2	9.2
0.0531	0.335	-	-	10.6	10.6
0.0690	0.5634	-	-	11.4	11.4
0.0992	1.166	-	-	6.8	6.8
0.1256	1.867	-	-	1.6 + 0.5	2.3
0.1674	3.320	0.33	0.2	0.29	0.8
0.1938	4.448	0.26	0.2	0.22	0.8
0.2281	5.162	0.32	0.2	0.32	0.8
0.2612	8.077	0.33	0.2	0.24	0.9
0.0677	0.5422	-	-	9.3	9.3

\* rounded to 0.1%

## 5. Automatic calibration of accelerometers

5.1 At the time when the calibrations described above were performed, the NMI automatic data logging and analysis system was not set up to perform calibrations of accelerometer-type sensors. Instead it was arranged to calibrate heave sensors whose output was, in general, a high pass filtered representation of the sensor's vertical position as a function of time. However, NMI are altering the system software in order to carry out accelerometer calibrations. The author's understanding of the proposed system is that it will operate in the same way as the heave calibration system. If this is the case, the data logging apparatus will be used to digitise 100 points on a single cycle of the accelerometer's output. The amplitude of the sine wave is then determined by performing a least squares fit to the data of a perfect sine wave.

Questions arise as to what accuracy might be expected from such a procedure, and as to whether a more accurate procedure could be adopted without undue complication of the system. There are two aspects of the proposed system which will be discussed in this context; firstly the adequacy of the sampling procedure, and secondly the more fundamental problem as to the desirability of using raw acceleration measurements without integrating the sensor's output.

5.2 Sampling Figs 2 and 3 show typical acceleration signals for frequencies below 0.12Hz. As may be seen in one case the high frequency noise is at about 50 times the rig frequency and in the other one the high frequency noise is about 25 times the rig frequency. Thus, from these considerations alone, sampling at 100 times the rig frequency is barely adequate as this corresponds to a nyquist frequency of 50 times the rig frequency. On careful examination of fig 3 it can be seen that much of the vibrational noise is nonsinusoidal so that higher frequency harmonics must be present, and a more rapid sampling scheme would be desirable.

5.3 Integration of Accelerometer signals The large uncertainties in the calibration, particularly at low angular frequencies, arise as a result of the relative sensitivity of accelerometers to high frequency vibrations. Thus it would seem sensible to apply a low pass filter to the data in order to reduce this effect. While almost any such filter with a

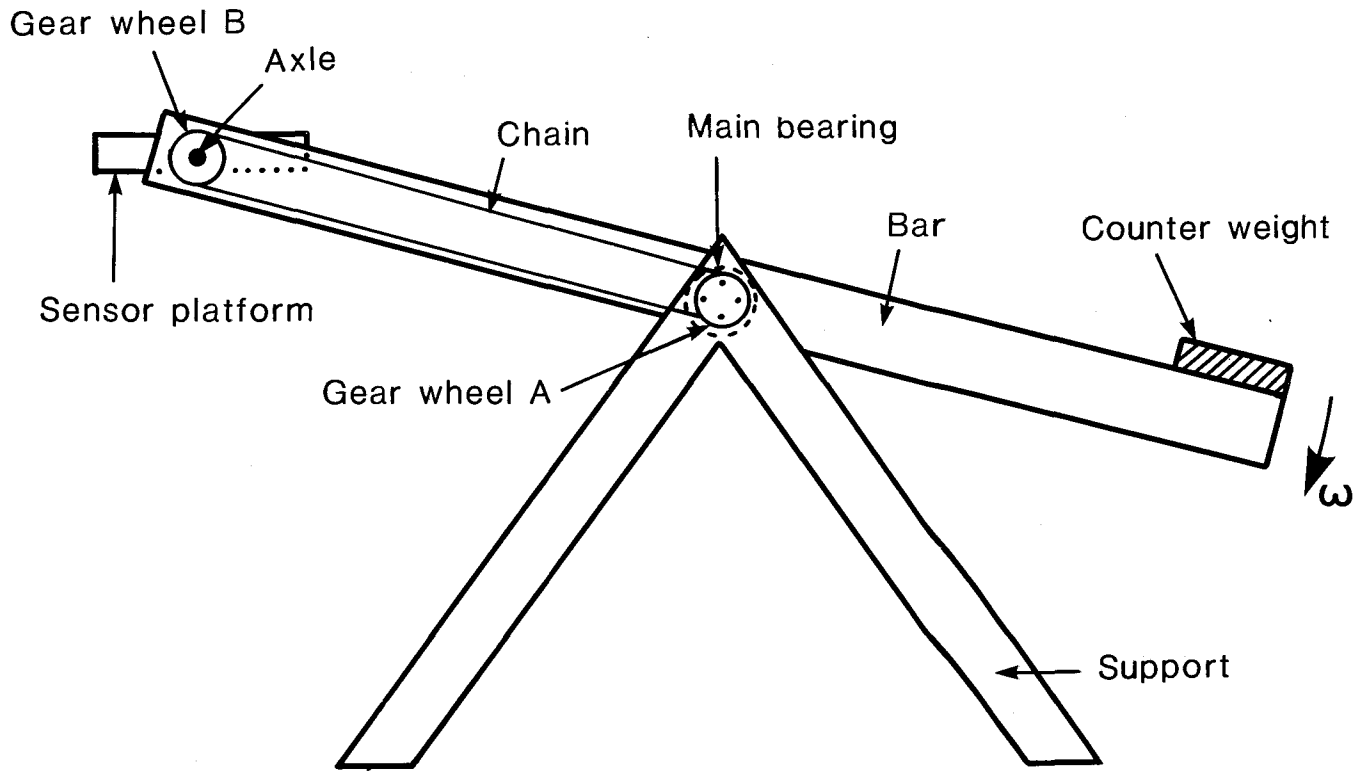
reasonably sharp cutoff could be used, there are particular advantages to using a double integrator for this purpose. Firstly such a procedure would give a filtered output which should, within limits, be independent of the rig frequency. This would make the interpretation of the data simpler. Secondly, such a system would be far less sensitive to variations in the rig's speed during the measurement. This is because, while the accelerations might vary in a complicated manner throughout one cycle, an accurate integrator must give a maximum amplitude equal to the length of the rotating arm. This process may also be thought of in terms of the system's sensitivity to variations in frequency.

In principle either analogue or digital integrators could be used with equivalent results. However, digital integrators would be preferable as, once such a system has been implemented, there is little possibility of inaccuracies in the calibration arising from a change in the integrator's characteristics. As a processor is already incorporated into the calibrator in order to fit a sine wave to the data, it should be possible to implement a simple digital integration procedure without altering the existing hardware.

## 6. Conclusions

The calibration of the accelerometers described above gives results which are consistent with a sensitivity in terms of output per unit acceleration which is close to that specified by the manufacturer, and is independent of frequency. For the interpretation of data derived from the buoys, the average of the measurements with angular frequencies above 0.04Hz is appropriate, giving average sensitivities of  $0.994 \text{ v/ms}^{-2}$  for sensor 18023 and 1.006 for sensor 18024. However, at low frequencies, a significant level of vibrational noise was recorded and this difficulty could be avoided if the accelerometer's output were double integrated prior to recording. This method also has the advantage that it is less dependant upon the rotational speed of the calibration rig.

Fig I  
Rotational Rig



The gear wheel A is fixed to the support frame while gear wheel B is connected by an axle to the sensor platform. As the Bar is driven at constant angular speed (using a drive system which is omitted for clarity), the sensor platform maintains a constant orientation in space while describing a vertical circle of 3m diameter.

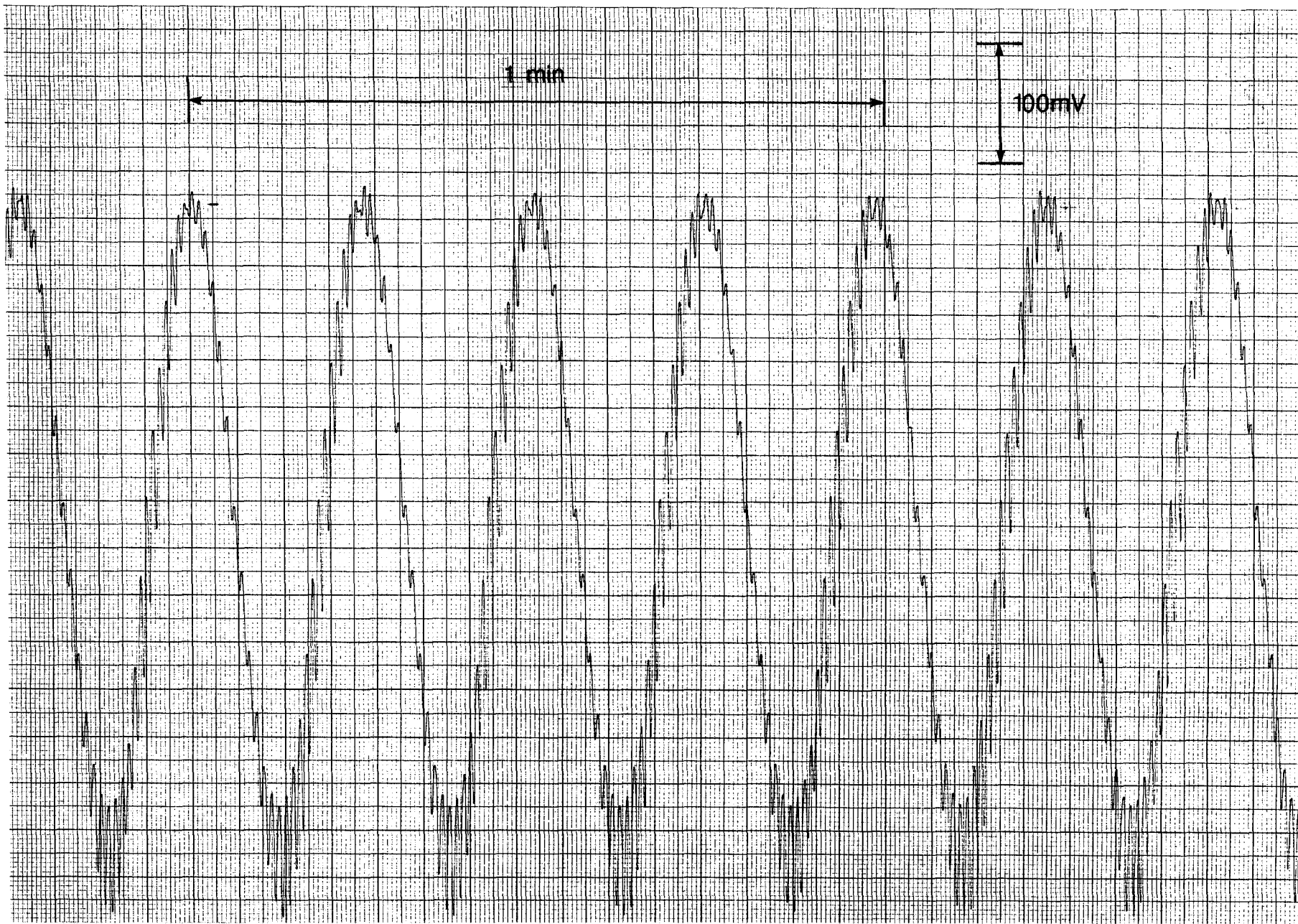


Fig 2: Accelerometer signal showing the effect of rig vibrations

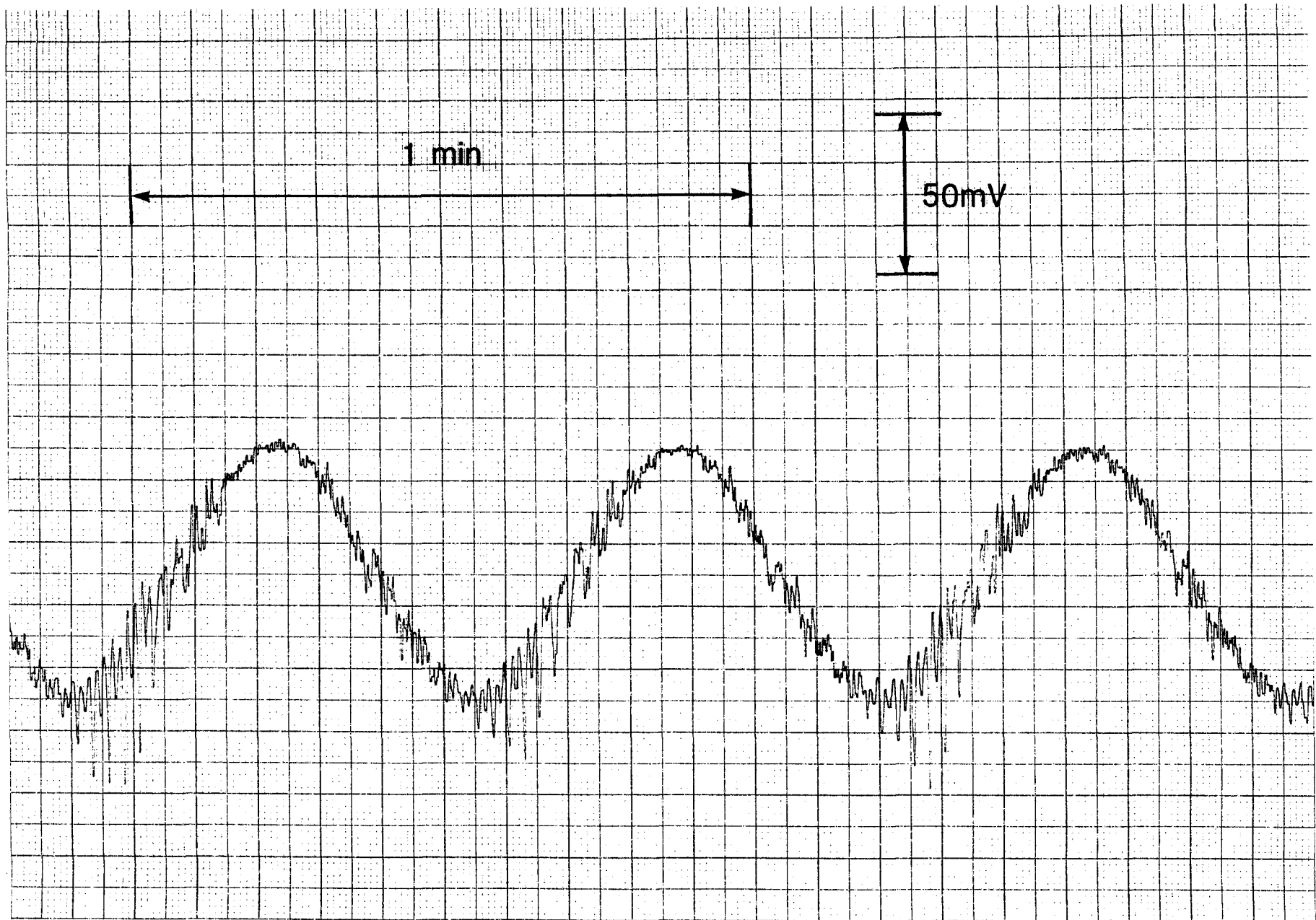


Fig 3: Accelerometer signal showing the effect of rig vibrations



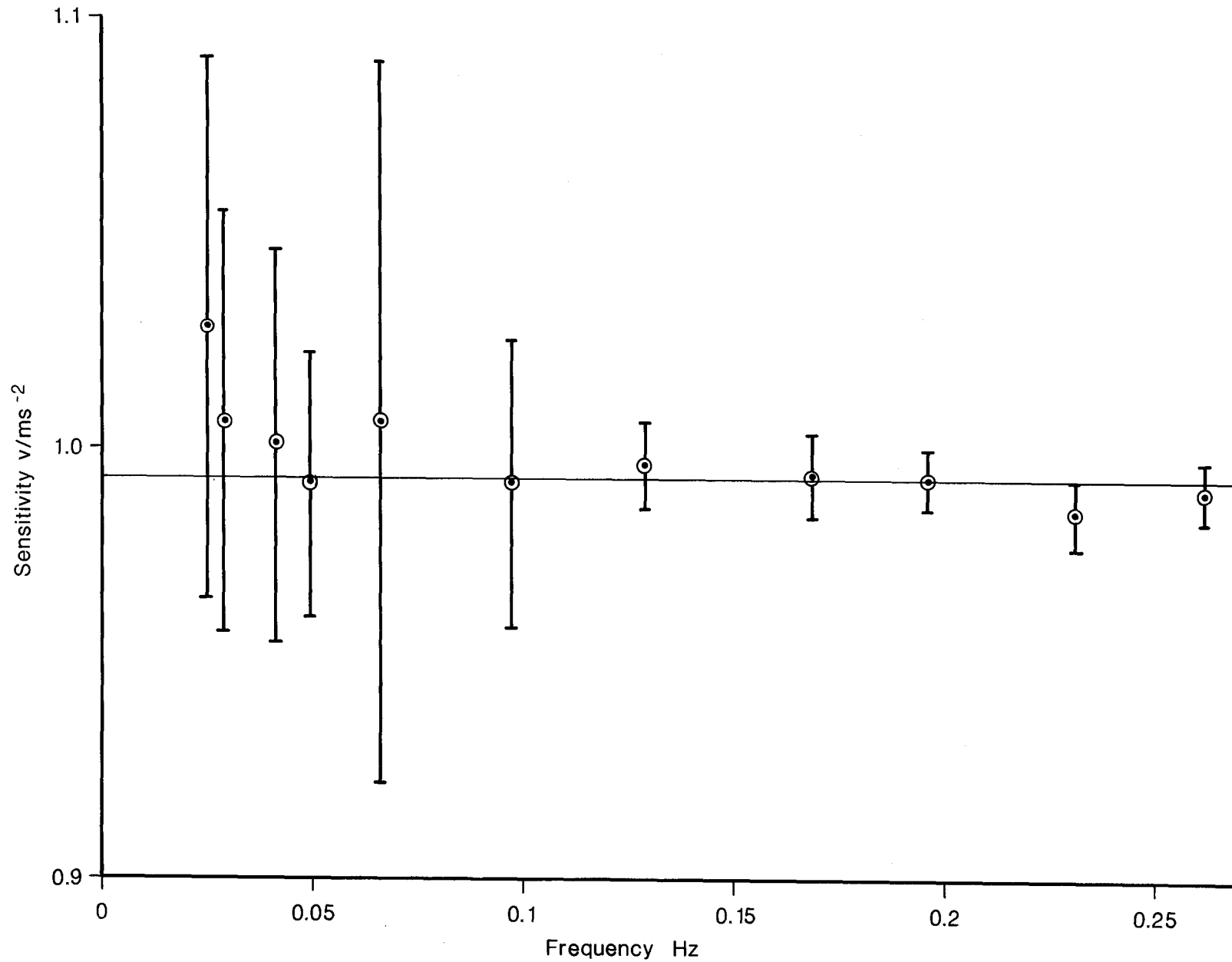


Fig 4: Calibration curve for sensor series No 18023 carried out on 4 November 1982  
The solid line corresponds to a sensitivity of 1.006 v/ms<sup>-2</sup>

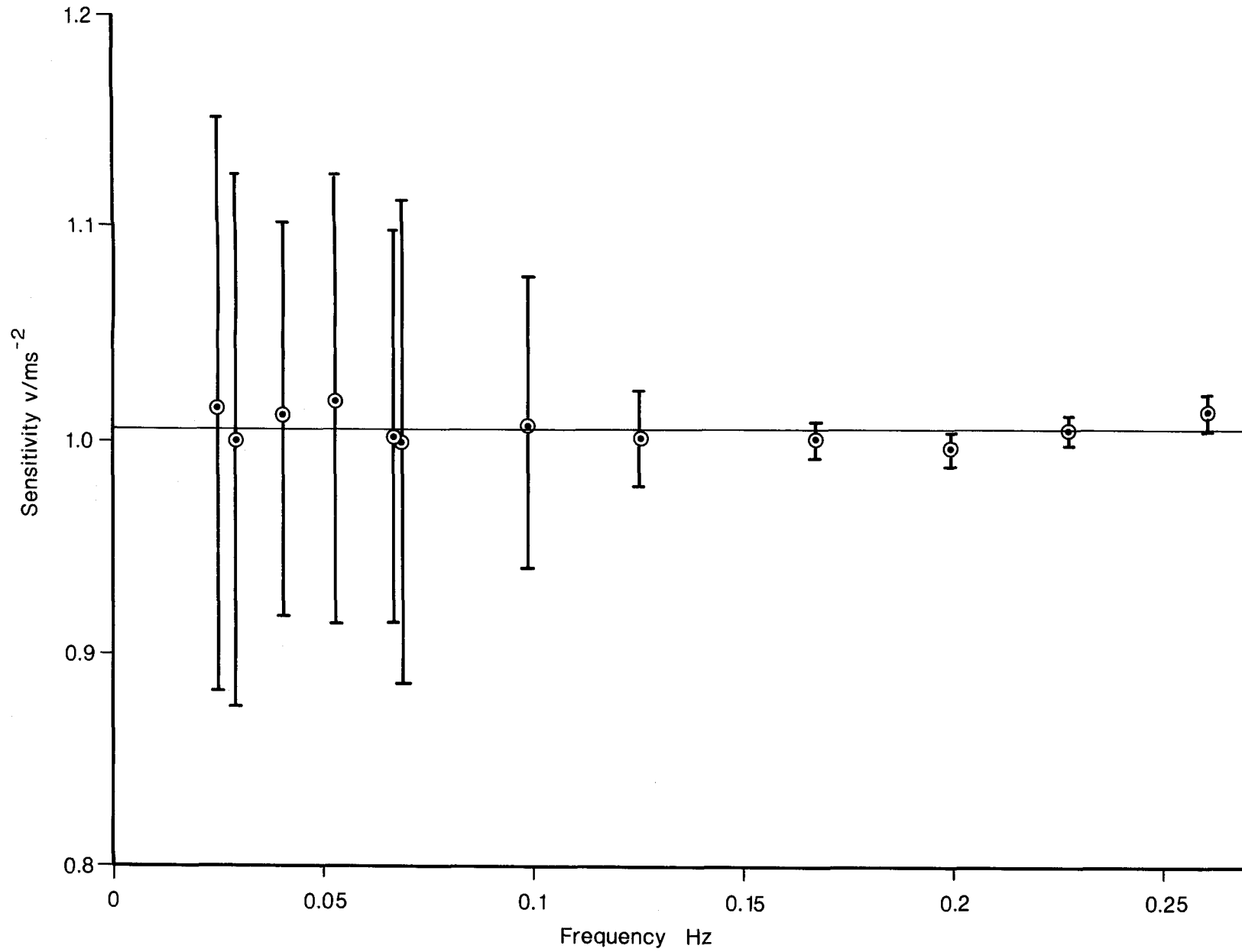


Fig 5: Calibration curve for sensor serial No 18024 carried out on 4 November 1982. The solid line corresponds to a sensitivity of 0.9935 v/ms<sup>-2</sup>

